FULL TITLE
ASP Conference Series, Vol. **VOLUME**, © **YEAR OF PUBLICATION**
NAMES OF EDITORS

Molecular Cooling as a Probe of Star Formation: Spitzer Looking Forward to Herschel

Edwin A. Bergin

Department of Astronomy, University of Michigan, 500 Church Street, Ann Arbor, MI 48109-1042

Sebastien Maret

Laboratoire d'Astrophysique de Grenoble, Observatoire de Grenoble, Université Joseph Fourier, CNRS, UMR 571, BP 53, F-38041 Grenoble, France

Yuan Yuan, Paule Sonnentrucker

Department of Physics and Astronomy, John Hopkins University, 3400 North Charles Street, Baltimore, MD 21218

Joel D. Green, Dan M. Watson

Department of Physics and Astronomy, University of Rochester, Rochester, NY 14627

Martin O. Harwit

Department of Astronomy, Cornell University, Ithaca, NY 14853-6801; and 511 H Street SW, Washington, DC 20024-2725

Lars E. Kristensen

Leiden Observatory, P.O. Box 9513 NL-2300 RA Leiden, The Netherlands

Gary J. Melnick, Volker Tolls

Harvard-Smithsonian Center for Astrophysics, 60 Garden Street, Cambridge, MA 02138

Michael W. Werner, Karen Willacy

Jet Propulsion Laboratory, California Institute of Technology, 4800 Oak Grove Drive, Pasadena, CA 91109

Abstract. We explore here the question of how cloud physics can be more directly probed when one observes the majority of cooling emissions from molecular gas. For this purpose we use results from a recent *Spitzer Space Telescope* study of the young cluster of embedded objects in NGC1333. For this study we mapped the emission from eight pure H_2 rotational lines, from $S(0)$ to $S(7)$. The H_2 emission appears to be associated with the warm gas shocked by the multiple outflows present in the region. The H_2 lines are found to contribute to 25 – 50% of the total outflow luminosity, and can be used to more directly ascertain the importance of star formation feedback on the natal cloud. From

these lines, we determine the outflow mass loss rate and, indirectly, the stellar infall rate, the outflow momentum and the kinetic energy injected into the cloud over the embedded phase. The latter is found to exceed the binding energy of individual cores, suggesting that outflows could be the main mechanism for cores disruption. Given the recent launch of *Herschel* and the upcoming operational lifetime of *SOFIA* we discuss how studies of molecular cooling can take a step beyond understanding thermal balance to exploring the origin, receipt, and transfer of energy in atomic and molecular gas in a wide range of physical situations.

1 Introduction

As the primary coolants molecules are key players in the thermal balance of gas in the dense interstellar medium (ISM). Our understanding of molecular cooling has a long history (see, for example Dalgarno and McCray 1972; Goldsmith and Langer 1978; Neufeld et al. 1995) and depending on the physical state the roster of potential key coolants extends well beyond CO to include water and a host of other molecular species. A key paper that truly demonstrates the richness and complexity of the issue was published in 1987 by Tom Phillips (Phillips 1987). A reproduction of the first figure in Phillips (1987) is shown here in Fig. 1, paired with the atmospheric transmission at the Atacama plateau.

A few things are notable: the scale of potential molecular cooling lines extends well beyond the millimeter-wave bands and into the sub-millimeter and far-infrared. The millimeter-wave spectrum is dominated by the emission from heavy species while the sub-millimeter/far-infrared is where lighter hydrides emit. Fig. 2 extends this picture illustrating the changes in the spectrum of molecular cooling as the physical and chemical state is altered. The warm ($T \sim 100 - 200$ K) hot core has a richer organic chemistry when compared to ambient gas. Because of the changes in the physical structure the emission spectrum at longer wavelengths in the hot core becomes densely packed with emission lines from large carbon-, hydrogen-, oxygen-, and nitrogen-bearing molecules. The higher temperature also excites higher energy transitions leading to strong emissions at shorter wavelengths. In contrast, the hot ($T > 500$ K) shocked gas can excite the weak quadrupole transitions of H_2 along with high energy transitions of CO, OH, and H_2O with the spectral emissions found primarily at far to mid-infrared wavelengths. Observing this entire spectrum of cooling and providing a spectral classification amongst objects is prohibited because the atmospheric is opaque at far-infrared wavelengths. In addition, the dust continuum emission is also strong and optically thick in the far-infrared hindering the detections of molecular emission. This can be overcome in part by wide band high spectral resolution observations which are only now coming into operation. These factors provide a primary motivation for *Herschel*, *SOFIA*, and *Spitzer* to name a few major missions.

Regardless, these figures clearly demonstrate that chemistry and physics are closely coupled. Furthermore the characteristics of the molecular emission directly probe the thermal state and therefore the energy input into the gas. In this paper we wish to explore the following question: *what can you do when you observe most (if not all) of the cooling luminosity?* In this regard we will focus

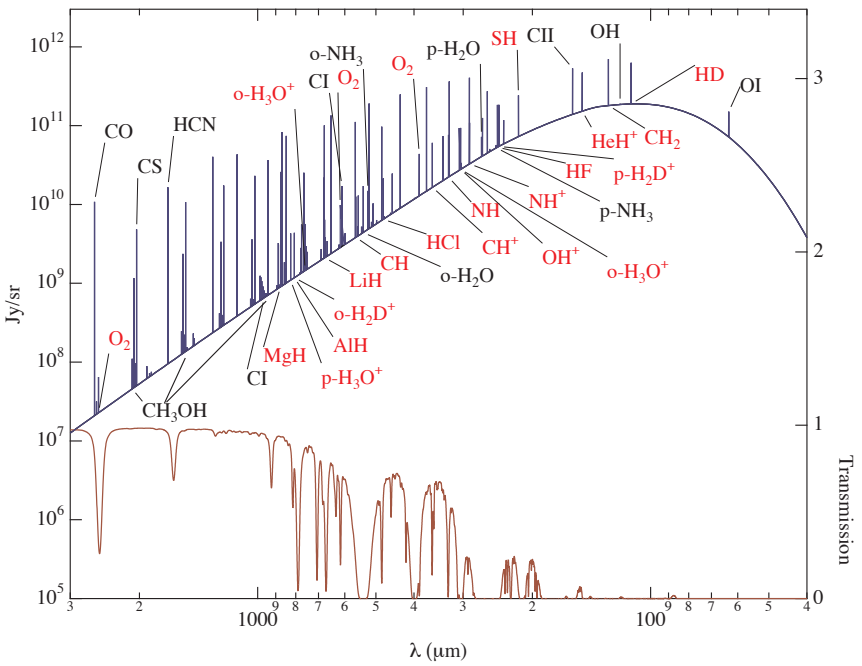

Figure 1. Predicted emission spectra from select species in the Orion Molecular Cloud. Figure is adapted from Phillips (1987) and illustrates the primary cooling lines in cold ambient gas. Species included are CH_3OH , H_2O , HCN, NH_3, OH, O I, O_2, H_2CO, CO, CS, HC_3N, and several hydrides (SH, HF, HCL, CH^+, LiH, H_2D^+, HD). Excitation from LVG calculations or LTE assuming a density of 10^5 cm^{-3}, temperature of 30 K, and column density of $N(H_2) = 4 \times 10^{22}$ cm^{-2}. Abundances taken from Blake et al. (1987). Also shown is the atmospheric transmission throughout the Far-IR estimated from the Atacama plateau.

on a recent series of observations of molecular hydrogen by the *Spitzer Space Telescope* published by Maret et al. (2009), but will end with some speculations on the near-term future now that *Herschel* has launched.

2 Spitzer Spectral Mapping of NGC1333

Using the *Spitzer-IRS* instrument we obtained complete spectral maps between $5.2 - 36.5$ μm toward the NGC1333 star-forming region in the Perseus cloud. This spectral region encompasses 8 rotational lines of molecular hydrogen, from S(0) to S(7) and several other fine structure lines from neutral and ionized metals (see e.g., Neufeld et al. 2006). The observations cover a region of roughly $6' \times 10'$, i.e. 0.4 pc $\times$ 0.5 pc assuming a distance of 220 pc (Cernis 1990). To our knowledge, these are the largest complete spectral maps obtained with the IRS. NGC 1333 contains many YSOs, revealed by sub-millimeter (Sandell & Knee 2001), millimeter (Lefloch et al. 1998) and mid-infrared continuum maps (Gutermuth et al. 2008). It also contains numerous molecular outflows, detected

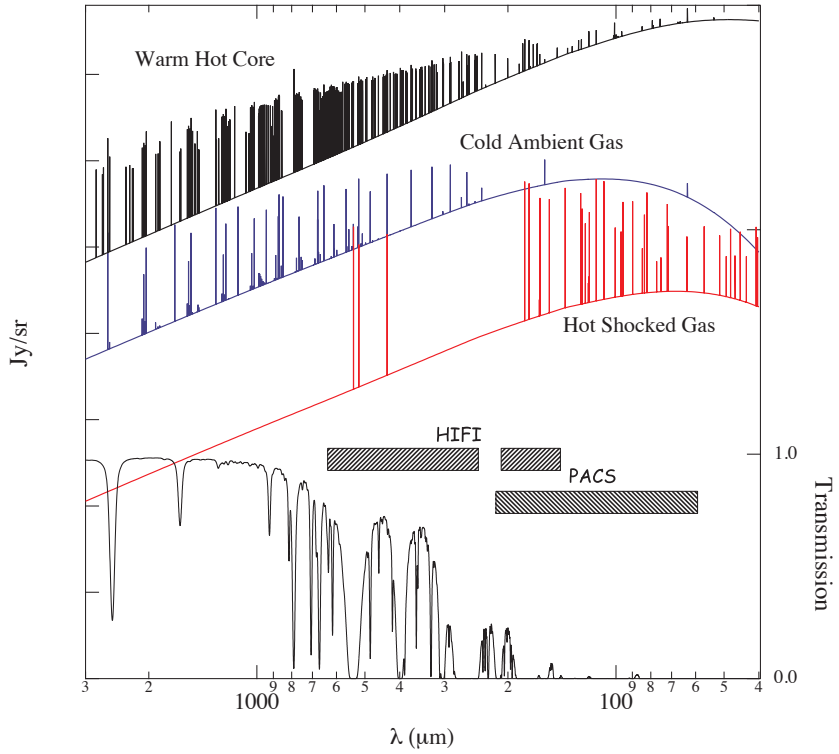

Figure 2. Predicted emission spectra from select species in the Orion Molecular Cloud with the Herschel HIFI and PACS wavelength coverage. Warm Hot Core and Cold Ambient Gas: species included are CH_3OH , H_2O , HCN, NH_3, OH, O I, O_2, H_2CO, CO, CS, HC_3N, and several hydrides (SH, HF, HCL, CH^+, LiH, H_2D^+, HD). Excitation from LVG calculations or LTE assuming a density of $n(H_2) = 10^7$ cm^{-3} and 10^5 cm^{-3}, temperatures of 100 K and 30 K, and column densities of $N(H_2) = 10^{23}$ cm^{-2} and 4×10^{22} cm^{-2} for the hot core and quiescent gas, respectively. Abundances taken from Blake et al. (1987). Shock fluxes are for O I, OH, H_2O, and H_2 and are taken from Kaufman & Neufeld (1996). Also shown is the atmospheric transmission throughout the Far-IR estimated from the Atacama plateau. The left-axis is unlabeled owing to the difference in emission scale between each of these components.

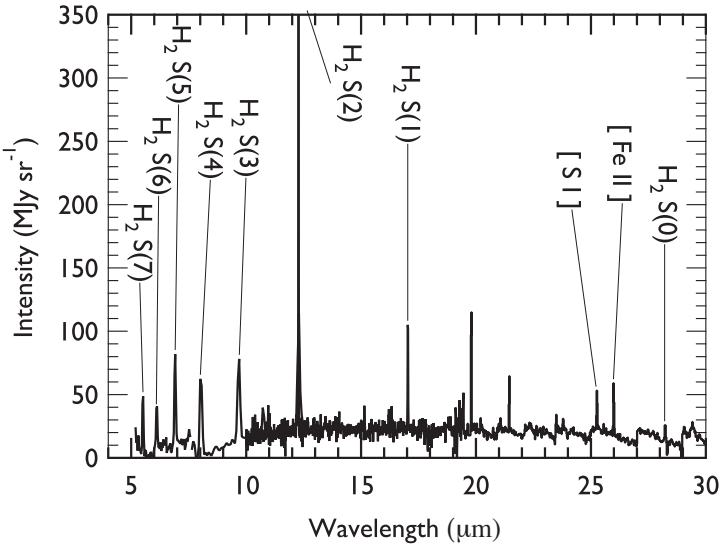

Figure 3. Sample IRS spectrum of shocked gas in NGC1333. Spectra taken towards HH7.

for example in CO line emission (Knee & Sandell 2000). Specifics regarding the instrument and observing modes are provided by Maret et al. (2009).

Fig. 3 shows a sample of the spectrum taken towards HH7 where we detect all 8 pure rotational transitions of H_2 that are in the band. Quadrupole transitions have low emission probabilities, thus this emission is optically thin; although it can suffer from wavelength dependent extinction from foreground material. Fig. 4 presents the spectral map of S(3), one of the strongest H_2 transitions. Several outflows appear prominent in the emission map including those associated with SVS13, IRAS 4A, IRAS 2A, IRAS 7, and SVS 13B. In each case we have mapped the entirety of the flow (with some gaps in coverage for the north-source flow associated with SVS13B) in all of the H_2 transitions accessible to *Spitzer*. Shock models of this emission are consistent with a mixture of non-dissociative shocks with $v_s \sim 20 - 30$ km s^{-1} (see §5.1 in Maret et al. 2009). The gas temperature varies with position as hotter gas does exist in some locations (e.g. HH7). Rotational diagrams find gas temperatures typically in the range of 300 – 1500 K. The transitions we have observed have upper state energies exceeding 7000 K and account for most of the luminosity carried by H_2 rotational emissions. The brightest transitions fall within the range with $J_{up} = 2 - 9$ covered by *Spitzer-IRS*. Thus we have covered the excitation peak for H_2 emission and know the total emissions of the dominant gas constituent over the entirety of 5 complete molecular outflows.

3 Molecular Cooling, Outflow Energy Loss, and Impact of Flow

In our *Spitzer* maps we have detected optically thin emission from eight rotational transitions of H_2 within these flows. Using these data, we can calculate

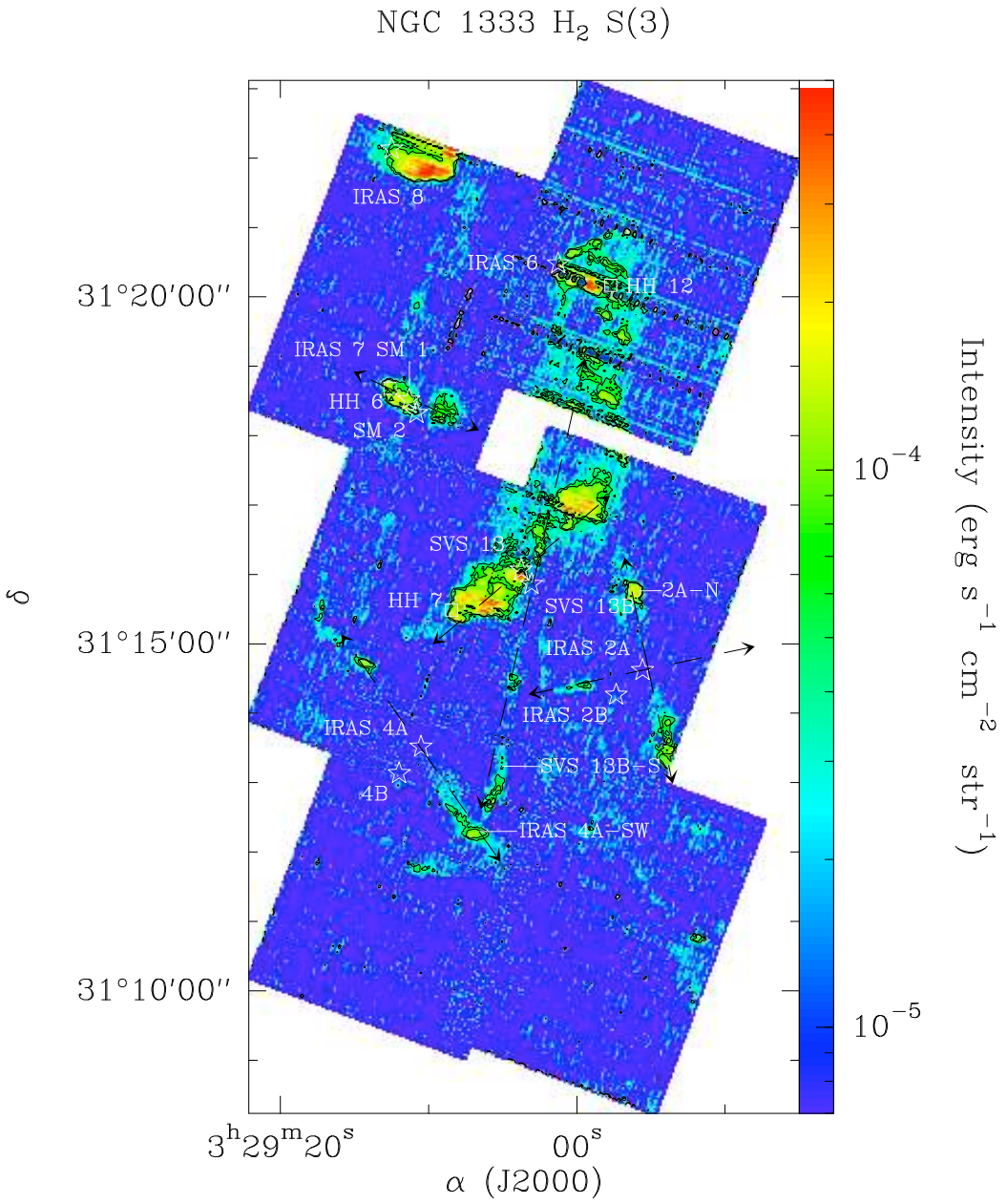

Figure 4. H_2 $S(3)$ continuum subtracted map obtained with the SL module. YSOs are indicated by open stars, while several HH objects are indicated by open squares. The outflows discussed in the text are indicated by dashed arrows. Contours show the 3, 5 and 10 σ noise levels. Figure taken from Maret et al. (2009) and reproduced by permission of the AAS.

the total H_2 luminosity in rotational emission, L_{H_2}, in the outflow by summing the emission over all rotational states and at each position within the region associated with each outflow. We provide the value of L_{H_2} for each flow in Table 3.2. The H_2 luminosity is related to the total outflow cooling rate by $L_{\rm tot} = \frac{1}{f_c} L_{H_2}$, where f_c is the fraction of the total cooling due to H_2 rotational emissions.

The shock models of Kaufman & Neufeld (1996) can be used to explore the contribution of H_2 to the overall cooling of the outflow via emission. Based on analysis of the H_2 emission, Maret et al. (2009) determine typical shock parameters of $n_0 \sim 10^4$ cm^{-3} and $v_s \sim 10-50$ km/s. Under these conditions Kaufman & Neufeld (1996) find that $f_c \sim 0.2 - 0.7$. The majority of H_2 cooling is via rotational lines, with only few percent contribution from H_2 vibrational emission. Note that in this source, the luminosity of the H_2 $1-0$ $S(0)$ ro-vibration line is 3×10^{-4} L$_\odot$ (Khanzadyan et al. 2003), well below the H_2 luminosity in rotational emission. The rest of the cooling flux arises from rotational, and to a lesser extent vibrational, lines of H_2O and CO, along with [O I] fine structure emission.

The *Infrared Space Observatory* has observed the primary cooling lines of CO, [O I], H_2O, OH, and H_2 with the SWS and LWS spectrometers in some of our sources. Molinari et al. (2000) observed HH 7 and compile the luminosities of the major cooling lines within the bandpass. For the HH 7 shock they find that 4.8×10^{-2} L$_\odot$ is released by O I, 2×10^{-2} L$_\odot$ by CO, 0.7×10^{-2} L$_\odot$ by H_2O, and 2.3×10^{-2} L$_\odot$ by H_2. However, the O I, CO, and H_2O observations were obtained using the LWS instrument with an $80''$ beam centered on HH 7, while the H_2 observations covered only the $S(1) - S(5)$ transitions within a $14'' \times 20''$ SWS beam. Our observations demonstrate that the H_2 emission extends well beyond the SWS aperture and the ISO SWS value is therefore a lower limit. We have convolved our data with a simulated $80''$ LWS beam and have recomputed the total luminosity of H_2 from $S(0) - S(7)$. We find that the H_2 luminosity in an $80''$ beam centered on HH 7 is 0.1 L$_\odot$. Combining the ISO observations with this revised value, we find that the H_2 provides about 50% of the total cooling ($f_c \sim 0.5$), in good agreement with models.

Information for other flows can be gleaned from the summary of ISO cooling lines of Giannini et al. (2001) which included two of our sources: the IRAS 2 north-south flow, and the IRAS 4A outflow. For these sources, we find (after adapting the results of Giannini et al. to our adopted distance of 220 pc) that $f_c \sim 0.25$. Using this information the total cooling luminosity of the outflows in NGC 1333 is approximately $L_{tot} \sim 2 - 4\ L_{H_2}$. For HH 7-11 we will adopt a $f_c = 0.5$ and for all other flows (which are not as prominent as HH 7-11) we adopt $f_c = 0.25$.

3.1 Determination of the stellar mass loss by outflows

The total energy loss generated by the outflow driven shock determined above is a direct measurement of the mechanical luminosity of the outflows. In this fashion, $\frac{1}{2}\dot{M}_o v_s^2 = (1-f_m) L_{tot} = (1-f_m)\frac{1}{f_c} L_{H_2}$, where $(1-f_m)$ is the fraction of shock mechanical energy that is translated into internal excitation, as opposed to translational motion. Kaufman & Neufeld (1996) estimate that $(1-f_m) \sim 0.75$ and we can then use the H_2 cooling emission to determine the outflow mass loss

rate, $\dot{M}_o$ from the young star. This equation can be simplified and placed in terms of the observed H_2 luminosity and estimated shock velocity:

$$\dot{M}_o \simeq 10^{-6}(1-f_m)\frac{1}{f_c}\left(\frac{L_{\rm H_2}}{10^{-2}\ L_\odot}\right)\left(\frac{v_s}{10\ {\rm km/s}}\right)^{-2}\ {\rm M_\odot\ yr^{-1}}. \quad (1)$$

In Table 1 we provide the observed H_2 luminosity, assumed shock velocity, and derived outflow properties.

In general we find that the outflows from the Class 0 protostars in the NGC 1333 cloud have values $\dot{M}_w \sim 0.6 - 2 \times 10^{-6}$ $M_\odot$ yr^{-1}. These values are comparable to values estimated in the literature (e.g. Bontemps et al. 1996; Giannini et al. 2001; Hatchell et al. 2007). In some cases measurements include sources within our sample. For example, Giannini et al. (2001) use FIR cooling lines towards IRAS 4 to derive $\dot{M}_w = 0.4-1.4\times10^{-6}$ $M_\odot$ yr^{-1} where we estimate $\dot{M}_w = 2 \times 10^{-6}$ $M_\odot$ yr^{-1}. The derived mass outflow rates can be related to the mass accretion rate ($\dot{M}_a$) using theoretical models of outflow generation. While the details and results can vary, a typical number is $\dot{M}_o \simeq 0.1\ \dot{M}_a$ (Pudritz et al. 2007), and our estimates provide $\dot{M}_a \sim 10^{-5}$ $M_\odot$ yr^{-1}. In this regard, Di Francesco et al. (2001) independently derived a mass infall rate of 1×10^{-4} $M_\odot$ yr^{-1} towards IRAS 4A using P Cygni spectral line profiles of H_2CO. In addition, Maret et al. (2002) derived an accretion rate of 5×10^{-5} $M_\odot$ yr^{-1} by modeling the FIR water lines emission from IRAS 4A and 4B envelopes. This is in reasonable agreement with our estimate of 2×10^{-5} $M_\odot$ yr^{-1} for this source.

It is useful to place our results in a broader context. Previous estimates of these quantities for molecular outflows have generally used velocity-resolved CO emission to provide a measure of the total H_2 mass in the flow, and used the velocity extent of the lines to trace the kinematics (e.g. Lada 1985; Bontemps et al. 1996). However, there are a number of uncertainties inherent in this method. The CO abundance has been calibrated to H_2 in some clouds (e.g. Frerking et al. 1982), but can vary if some CO remains frozen on grains (e.g. Bergin & Tafalla 2007) or is photodissociated by radiation generated in the shock or leaking through the outflow cavity. In addition, the CO molecules can be excited in both the low temperature natal core and in the warmer outflow. Thus towards the central core the spectral line contains a mixture of emission from the high velocity dispersion core and low dispersion core. To some extent these components can be disentangled, but there is significant uncertainty regarding the outflow mass present at low velocities that also correspond to the core (Lada & Fich 1996). CO emission itself is often optically thick, even in the extended line wings. Observations of isotopologues are therefore required, but not always available to correct for the effects of optical depth (e.g. Yu et al. 1999; Arce & Goodman 2001). Finally, estimates of the CO velocities are dependent on the outflow inclination. In a handful of cases, this can be directly measured if proper motion data can be used to measure the tangential velocity to compare to the observed radial velocity in the spectral lines. In the majority of cases this information is not available, and inclinations have instead been estimated by models of the flow velocity at different inclinations compared to the observed emission distribution (e.g. Cabrit et al. 1988). However, this estimate is also uncertain.

Our measurements do not suffer from any of these uncertainties. The H_2 lines are optically thin and our observations encompass the most emissive H_2 rotational lines, which we simply sum over rotational states and positions to derive the total emission. We have used shock models to calibrate the amount of cooling accounted for by other molecules. In 3 sources covered by our maps, we have confirmed that the models are accurately reproducing the observed distribution of cooling power. Since H_2 is the dominant species and a primary coolant we are directly tracing the energy loss in the most abundant species. H_2 does not emit within the core itself and thus we have no line of sight contamination. By using the cooling luminosity to trace outflow energetics our measurements are completely independent of the outflow inclination. As an example our momentum flux estimates are a factor of $\sim 4-8$ above values – uncorrected for inclination – derived from CO emission in same flows in NGC 1333 (Hatchell et al. 2007). On the other hand, our estimates are in good agreement the values (corrected for inclination) of Sandell & Knee (2001).

Our conclusion is similar to that of Giannini et al. (2001) who used ISO observations of FIR cooling lines as a measure of the total mechanical luminosity. The major difference is that we use spatially resolved observations of H_2 and supplement our results with those of Giannini et al. (2001) to derive the total cooling loss. Given that we have observed the major coolants, the primary uncertainty in the mass loss rate derivation is the assumed shock velocity. The expected range of shock strengths to create the observed H_2 emission is $\sim$10 – 50 km/s, with adopted values of $\sim 20-30$ km/s (Maret et al. 2009). We therefore estimate that the mass outflow rate values are accurate to within a factor of 3 (given a distance of 220 pc).

3.2 Impact of flow on natal core

It is well known that outflows inject significant energy and momentum in the the surrounding cloud (e.g. Lada 1985; Arce et al. 2007; Davis et al. 2008) with some suggestions that these flows drive supersonic motions (Quillen et al. 2005). It is also possible that the outflow is the key player in the disruption of the natal core (e.g. Tafalla & Myers 1997; Fuente et al. 2002). Our data offer a new opportunity to explore the question of the outflow impact on the surrounding material in the specific case of low mass star formation.

The total momentum injected by outflows into a core is given by $P = \dot{P}\,\tau_{dyn}$ ($M_\odot$ km s^{-1}), where τ_{dyn} is the outflow dynamical timescale. Using τ_{dyn} values from Knee & Sandell (2000), we find P values ranging from 0.1 to 0.4 $M_\odot$ km s^{-1} (see Table 3.2). If a similar level of outflow activity persists during the lifetime of the embedded phase of $\sim 5\times10^5$ yrs (Evans et al. 2009) then the total momentum over this phase is $\sim 4-20$ $M_\odot$ km s^{-1}. There is some evidence in the literature of a decline in the outflow momentum flux during the transition from Class 0 to Class I (Bontemps et al. 1996). However, Hatchell & Fuller (2008), with a homogeneous sample of sources in Perseus, do not confirm this result, finding similar momentum fluxes for sources with comparable luminosities and masses.

Based on these estimates when the entrained outflowing material slows down to 1 km s^{-1} it will have swept up $4-20$ $M_\odot$ of material. Assuming a typical core mass of ~ 5 $M_\odot$ then the outflow is clearly capable of destroying the core during the lifetime of the embedded phase. Of course, the flow will only dis-

perse material in its path and the typical outflow cone angle in these sources is $\sim 60^{\circ}$ (Jørgensen et al. 2007). However, observations suggest that the outflow cone angle increases with age (Velusamy & Langer 1998; Arce & Sargent 2006). Estimates of core masses vary by nearly an order of magnitude in the literature (Lefloch et al. 1998; Sandell & Knee 2001; Walsh et al. 2007) so definitive comparisons within our small sample are difficult. Nonetheless these data clearly suggest that the outflow could be the main mechanism for core dispersal.

To support our assertion that the transfer of outflow momentum to the core is a main mechanism for core dispersal we can also compare the energetics. Tafalla & Myers (1997) demonstrated that the outflow from a massive star (Mon R2) exceeds or is comparable to the gravitational binding energy of its core. Thus the Mon R2 outflow has likely sculpted that object. However, massive star outflows are more energetic than the low mass objects sampled in our maps and this result may not scale to low mass systems. The average total energy generated by the current generation of outflows in the center of NGC 1333 is $\langle L_{H_2}/f_c \times \tau_{dyn} \rangle = 2 \times 10^{43}$ ergs. The gravitational binding energy of a sphere is $\alpha\, GM^2/R$ with $\alpha = 1$ for cores with a r^{-2} density profile (MacLaren et al. 1988), as expected for these embedded protostars. For a typical core mass of ~ 5 $M_{\odot}$ and radius of 0.03 pc the binding energy is $\sim 4 \times 10^{43}$ ergs. If we assume that a similar level of activity exists over the lifetime of the embedded phase then the outflow energetics are equal to or even exceed the gravitational energy of the core. In sum, both the flow energetics and momentum suggest that outflows are the primary method for core dispersal. Molecular gas observations show that the NGC 1333 cores discussed here are embedded in a much larger but lower density cloud (e.g. Pineda et al. 2008). As typical for GMCs, the cloud binding energy is much greater than those of each individual cores. Thus the flows which disrupt the cores are not major players in cloud disruption as the cloud momentum and energy far exceed that provided by the current generation of flows over their lifetime.

Table 1. Outflow Properties

Source	L_{H_2} (10^{-2} $L_{\odot}$)	f_c	v_s (km/s	$\dot{M}_w$ ($M_{\odot}$yr^{-1})	$\dot{P}$ ($M_{\odot}$yr^{-1}km s^{-1})	τ^a_{dyn} (yr)	P ($M_{\odot}$km s^{-1})
HH 7-11	11.1	0.50	26	2×10^{-6}	5×10^{-5}	5600	0.29
IRAS 4A	1.8	0.25	16	2×10^{-6}	3×10^{-5}	12000	0.38
IRAS 2^b	1.5	0.25	28	6×10^{-7}	2×10^{-5}	17000	0.34
IRAS 7	1.8	0.25	34	5×10^{-7}	2×10^{-5}	5700	0.11
SVS 13B	0.8	0.25	19	7×10^{-7}	2×10^{-5}	22000	0.44

4 Conclusion and Future Prospectus

We have presented here the results from an analysis of observations of the pure rotational emission lines of molecular hydrogen in several molecular outflows in the NGC1333 molecular cloud. These observations have demonstrated the power of observing the emission from the majority of coolants within shocked gas. From these emissions we were able to explore total mechanical energy input arising in energetic outflowing gas from the young forming star and into the natal cloud. Based on our estimates we find that the outflow is likely the primary mechanism for core disruption.

Exploring Figs. 1 and 2 many of the key coolants of colder regions in the ISM lie in the far-infrared. These include water and other light hydrides but also the host of molecular emission from complex species which contribute in dense regions (see Neufeld et al. 1995). *Herschel* and within a few years *SOFIA*, will offer tremendous coverage of this key wavelength regime. This offers us a new ability to follow the energy content of molecular gas over a wide range of temperature regimes. For example, in our study of shocked gas given above, we utilized results from a similar ISO study of young class 0 objects (Giannini et al. 2001) to understand the contributions from O I and C II. Fine structure emissions of these two atoms are primary coolants of the general ISM and also will be important as coolants in molecular gas exposed to strong radiation fields. This includes gas exposed to radiation from external stars (photodissociation regions; Tielens and Hollenbach 1985), but also flared protoplanetary disks (Nomura et al. 2007). In these systems we can begin to explore the energy input from radiation and its transfer within the atomic and molecular layers more directly than assuming a value of G_0. In molecular outflows, maps of key coolants can be combined with *Spitzer* data to determine the total energy loss with its relation to mass loss, with no need for a correction factor. In all the new access to this crucial wavelength regime enables studies of molecular cooling to take a step beyond understanding thermal balance to exploring the origin, receipt, and transfer of energy in molecular gas.

Acknowledgments. This work is based on observations made with the Spitzer Space Telescope, which is operated by the Jet Propulsion Laboratory, California Institute of Technology under a contract with NASA. Support for this work was provided by NASA through an award issued by JPL/Caltech for program #20378. EAB would also like to gratefully acknowledge significant support, including involvement with the Herschel mission, and advice from T. Phillips throughout his career.

References

Arce, H. G. & Goodman, A. A. 2001, ApJ, 554, 132
Arce, H. G. & Sargent, A. I. 2006, ApJ, 646, 1070
Arce, H. G., Shepherd, D., Gueth, F., Lee, C.-F., Bachiller, R., Rosen, A., & Beuther, H. 2007, in Protostars and Planets V, ed. B. Reipurth, D. Jewitt, & K. Keil, 245–260
Bergin, E. A. & Tafalla, M. 2007, ARA&A, 45, 339
Blake, G. A., E. C. Sutton, C. R. Masson, and T. G. Phillips 1987. ApJ315, 621-645.
Bontemps, S., Andre, P., Terebey, S., & Cabrit, S. 1996, A&A, 311, 858
Cabrit, S., Goldsmith, P. F., & Snell, R. L. 1988, ApJ, 334, 196
Cernis, K. 1990, Ap&SS, 166, 315
Dalgarno, A. and R. A. McCray 1972. ARA&A10, 375.
Davis, C. J., Scholz, P., Lucas, P., Smith, M. D., & Adamson, A. 2008, MNRAS, 387, 954
Di Francesco, J., Myers, P. C., Wilner, D. J., Ohashi, N., & Mardones, D. 2001, ApJ, 562, 770
Evans, N. J. et al. 2009, ApJS, 181, 321
Frerking, M. A., Langer, W. D., & Wilson, R. W. 1982, ApJ, 262, 590
Fuente, A., Martın-Pintado, J., Bachiller, R., Rodrıguez-Franco, A., & Palla, F. 2002, A&A, 387, 977
Giannini, T., Nisini, B., & Lorenzetti, D. 2001, ApJ, 555, 40

Goldsmith, P. F. and W. D. Langer 1978. ApJ222, 881-895.
Gutermuth, R. A., Myers, P. C., Megeath, S. T., Allen, L. E., Pipher, J. L., Muzerolle, J., Porras, A., Winston, E., & Fazio, G. 2008, ApJ, 674, 336
Hatchell, J. & Fuller, G. A. 2008, A&A, 482, 855
Hatchell, J., Fuller, G. A., & Richer, J. S. 2007, A&A, 472, 187
Jørgensen, J. K., Bourke, T. L., Myers, P. C., Di Francesco, J., van Dishoeck, E. F., Lee, C.-F., Ohashi, N., Schöier, F. L., Takakuwa, S., Wilner, D. J., & Zhang, Q. 2007, ApJ, 659, 479
Kaufman, M. J. & Neufeld, D. A. 1996, ApJ, 456, 611
Khanzadyan, T., Smith, M. D., Davis, C. J., Gredel, R., Stanke, T., & Chrysostomou, A. 2003, MNRAS, 338, 57
Knee, L. B. G. & Sandell, G. 2000, A&A, 361, 671
Lada, C. J. 1985, ARA&A, 23, 267
Lada, C. J. & Fich, M. 1996, ApJ, 459, 638
Lefloch, B., Castets, A., Cernicharo, J., Langer, W. D., & Zylka, R. 1998, A&A, 334, 269
MacLaren, I., Richardson, K. M., & Wolfendale, A. W. 1988, ApJ, 333, 821
Maret, S., and 12 colleagues 2009. ApJ698, 1244-1260.
Maret, S., Ceccarelli, C., Caux, E., Tielens, A. G. G. M., & Castets, A. 2002, A&A, 395, 573
Molinari, S., Noriega-Crespo, A., Ceccarelli, C., Nisini, B., Giannini, T., Lorenzetti, D., Caux, E., Liseau, R., Saraceno, P., & White, G. J. 2000, ApJ, 538, 698
Neufeld, D. A., Melnick, G. J., Sonnentrucker, P., Bergin, E. A., Green, J. D., Kim, K. H., Watson, D. M., Forrest, W. J., & Pipher, J. L. 2006, ApJ, 649, 816
Neufeld, D. A., S. Lepp, and G. J. Melnick 1995. ApJS100, 132.
Nomura, H., Y. Aikawa, M. Tsujimoto, Y. Nakagawa, and T. J. Millar 2007. ApJ661, 334-353.
Phillips, T. G. 1987. Interstellar Processes 134, 707-730.
Pineda, J. E., Caselli, P., & Goodman, A. A. 2008, ApJ, 679, 481
Pudritz, R. E., Ouyed, R., Fendt, C., & Brandenburg, A. 2007, in Protostars and Planets V, ed. B. Reipurth, D. Jewitt, & K. Keil, 277–294
Quillen, A. C., S. L. Thorndike, A. Cunningham, A. Frank, R. A. Gutermuth, E. G. Blackman, J. L. Pipher, and N. Ridge 2005. ApJ632, 941-955.
Sandell, G. & Knee, L. B. G. 2001, ApJ, 546, L49
Tafalla, M. & Myers, P. C. 1997, ApJ, 491, 653
Tielens, A. G. G. M. and D. Hollenbach 1985. ApJ291, 722-754.
Velusamy, T. & Langer, W. D. 1998, Nat, 392, 685
Walsh, A. J., Myers, P. C., Di Francesco, J., Mohanty, S., Bourke, T. L., Gutermuth, R., & Wilner, D. 2007, ApJ, 655, 958
Yu, K. C., Billawala, Y., & Bally, J. 1999, AJ, 118, 2940